

Strong motion data analysis of the 4 April 2011 Western Nepal earthquake (M 5.7) and its implications to the seismic hazard in the Central Himalaya

Naresh Kumar* and D. D. Khandelwal

Wadia Institute of Himalayan Geology, 33 GMS Road, Dehradun 248 001, India

In the present study, the strong motion data of the 4 April 2011 western Nepal earthquake (M 5.7) recorded by a dense network of 24 strong motion accelerograph stations have been used to estimate horizontal and vertical component of the peak ground acceleration (PGA) to better understand its bearing on the seismic hazard scenario of the Central Himalayan region. We assimilated attenuation curves using the observed PGA values and found that the zone is associated with higher H/V ratio in which the attenuation trend remains bimodal with one trend for closer distance up to 100–120 km, while the other trend corresponds to distances extending beyond 1000 km. We infer that the two different PGA trends have close bearing on the major tectonics and structural set-up of the region, which is possibly attributed to subsurface structural variation through which the seismic wave travels, suggesting changes of crustal heterogeneities beneath the source zone. The present work may improve the concept of ground motion model for evaluating seismic hazard for the Himalaya.

Keywords: Earthquakes, peak ground acceleration, seismic hazard, strong motion data.

WESTERN Nepal and the adjoining parts of Garhwal and Kumaun of Central Himalaya (Figure 1) are seismically the most active zones located on the inter-plate boundary of the Indian and Eurasian tectonic plates. The concentration of moderate magnitude earthquakes (Figure 2) is high for the Garhwal and Kumaun regions of western Himalaya^{1,2} compared to adjoining parts of the Himalayan region. The region has a complex tectonic setting^{3–5} with a highly deformed upper crust due to ongoing tectonic movements. This part of the Himalaya is prone to the occurrence of strong and large earthquakes as evidenced in the past. For example, the 1991 Uttarkashi (M 6.5) and 1999 Chamoli (M 6.6) which occurred on the western side (Figure 2) to the epicentre of the 4 April 2011 Western Nepal earthquake (M 5.7). In addition, two

great earthquakes occurred on either side of Central Himalaya, the 1905 Kangra earthquake (M 7.8) towards its west and the 1934 Bihar earthquake (M 8.3) to the east^{6–8}. The epicentre locations and rupture zones of these two great earthquakes imply the existence of a wide seismic gap in the Central Himalaya where great or large earthquakes did not occur. The recent disastrous Nepal earthquake of 25 April 2015 earthquake (M_w 7.8) has reduced a small part of this seismic gap from the eastern side. However, according to Mishra⁹, the reoccurrence interval of great Himalayan earthquakes is quite uncertain and the seismic gap theory needs thorough investigation. Since we do not have proper assessment of what type of

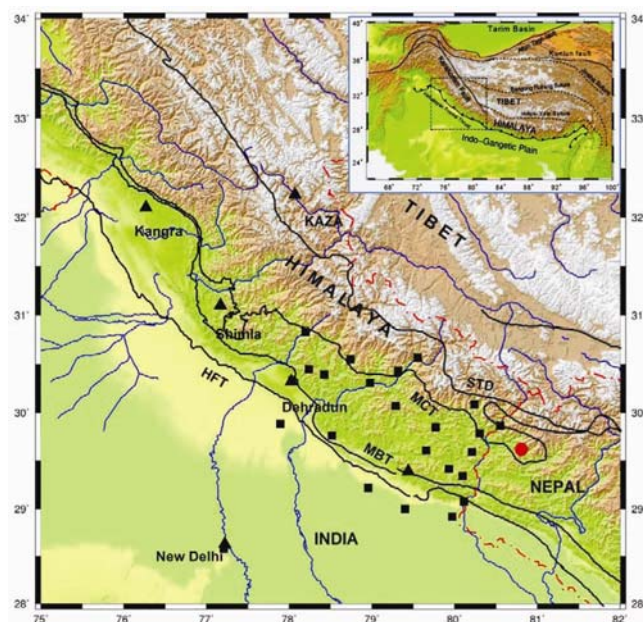


Figure 1. Tectonic map along with data collection stations and epicentre of the earthquake. Epicentre of the 4 April 2011 Nepal earthquake (M 5.7) is shown with a red circle; strong motion stations are shown with black rectangle and some important places are shown with black triangle. (Inset) Map of Himalaya–Tibet region; the present study region is shown with the dotted rectangle. HFT, Himalayan Frontal Thrust; MBT, Main Boundary Thrust; MCT, Main Central Thrust; STD, South Tibetan Detachment.

*For correspondence. (e-mail: nkd@wihg.res.in)

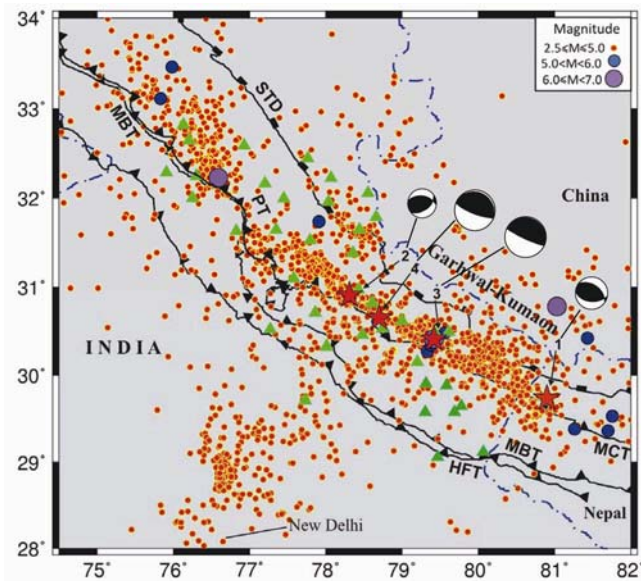


Figure 2. Recent seismic activity of NW Himalaya (modified after Kumar *et al.*)²; epicentres and recording seismic stations shown using filled circles and triangles respectively. The locations (stars) and focal mechanisms (beachball) of four recent strong earthquakes are (1) 2011 Nepal (M 5.7), (2) 2007 Kharsali (M 5.0), (3) 1999 Chamoli (M 6.6) and (4) 1991 Uttarkashi (M 6.4).

structural heterogeneities prevail beneath the seismic gap zones. Therefore, a detailed study of the region is important for assessment of seismic hazards.

The seismic activity in the region is mainly confined in the plate boundary zone with highest concentration in the central part aligned nearly to the eastwest extended Himalayan arc. It is mainly caused by the under-thrusting of the Indian plate beneath the Eurasian plate in the Himalayan part where the down-going Indian plate has detachment contact with the Himalayan wedge¹⁰; the contact is described as the Main Himalayan Thrust (MHT). The seismicity is high around the surface trace of the Main Central Thrust (MCT), which is the central part of nearly eastwest extended Himalayan mountain zone. This high seismic activity zone is described as the main Himalayan seismic belt concentrated around MCT (Figure 2) that can be linked with the major thrusts and transverse faults of the region with the southern boundary as the Main Boundary Thrust (MBT)⁶. In addition, several local tectonic faults are aligned transverse to the trend of the Himalaya which has been active since the Late Tertiary³, these can also be allied with seismic activity. Gitis *et al.*¹¹ have associated the occurrence of large magnitude earthquakes with high elevation relief in the NW Himalaya, indicating these are due to subsurface features.

The available fault plane solutions (FPS) of this central part of the Himalaya and in general the entire Himalayan arc compel us to mark the tectonic fault as thrusts dipping towards northeast^{6,12–14}. The available solutions of two strong earthquakes of this region, the 1991 Uttarkashi (M 6.5) and the 1999 Chamoli (M 6.6), the recent works

in Nepal Himalaya¹⁴, Garhwal Himalaya², the solutions from USGS for past earthquakes and present solution of the 4 April 2011 western Nepal earthquake (M 5.7) also suggest thrust dominance mechanisms. Strong motion data are widely used throughout the globe for seismic hazard evaluation and development of attenuation relations for strong motion^{15–19}. Review of attenuation relations highlights their existence worldwide, which is refined and modified with the introduction of new data and also incorporated for other regions²⁰. Peak ground acceleration (PGA) is an important parameter for incorporation of attenuation relations to be utilized for the study of structure safety²¹ and mitigation of seismic hazard.

The strong motion earthquake data are useful for the evaluation of seismic hazard to the high-risk zones situated on the platform of intense seismic activity (Figure 2). Also, it becomes necessary while considering a zone of wide seismic gap. The 4 April 2011 western Nepal earthquake (M 5.7) is a significant event for the study region because during the occurrence of this earthquake, the strong motion data were recorded at many stations on the local network. Based on the present dataset of 23 stations (Table 1), we incorporate the attenuation relations, refine the available attenuation curves and compare the results with other parts of the Himalaya and the world. The evaluated attenuation relations are further utilized for assessing the residuals from the model curves and the observed values may be useful for the seismic hazard evaluation. Also, horizontal-to-vertical component (H/V) ratios are obtained from recording sites to further enhance the usefulness of the dataset.

Strong motion array and data acquisition

The Earthquake Engineering Department at the Indian Institute of Technology Roorkee (IITR), has installed three strong motion arrays in the Himalayan region^{19,22–24}. One array is in the Central Himalaya, which is a dense local network of 40 accelerographs out of total 300 in the entire Himalayan region. As shown in Figure 1, these stations in the Central Himalaya are installed in the Indian part to the west of Nepal. The stations are well-equipped and cover the parts of Central Himalaya, including major and local tectonic features where the seismic activity is high. The digital equipment from Switzerland are GeoSIG, triaxial force balanced accelerometer and 18-bit digitizer²³; Table 2 provides the detailed information. The time synchronization is through attached Global Positioning System (GPS). The data are recorded in trigger mode at the time of occurrence of strong earthquakes, whenever the acceleration of the recording site exceeds 0.002 g level. During the occurrence of strong earthquake, the data are recorded by three components at a sampling rate of 200 SPS. The epicentre of the 4 April

Table 1. The peak ground acceleration (PGA) recorded at different stations

Station	Latitude (°N)	Longitude (°E)	Elevation (m)	PGA E-W (cm/s ²)	PGA N-S (cm/s ²)	PGA VT (cm/s ²)	Distance (km)	Site type
Almora	29.596	79.657	1642	9.662	10.662	7.588	110.5	A
Bageshwar	29.831	79.770	972	10.856	9.857	4.310	102.7	A
Barkot	30.809	78.205	1305	7.816	6.078	2.512	283.3	A
Chamoli	30.412	79.320	1578	11.124	17.466	8.763	168.7	A
Champawat	29.334	80.095	1635	31.551	17.078	10.636	74.38	A
Dehradun	30.316	78.042	662	3.165	3.288	1.535	277.4	C
Dhanaulti	30.427	78.244	2280	7.454	7.209	2.138	262.7	B
Dharchula	29.847	80.546	909	131.811	131.634	56.222	36.82	A
Didihat	29.770	80.300	1720	16.350	18.821	12.680	51.87	A
Garasain	30.051	79.288	1614	20.355	19.236	12.845	154.2	A
Joshimath	30.546	79.555	1919	10.911	10.275	5.597	159.4	A
Kashipur	29.211	78.960	216	8.823	10.254	7.219	183.4	C
Khatima	28.919	79.969	215	25.813	20.830	8.320	110.6	C
Kothdwar	29.748	78.523	389	6.413	4.099	4.123	220.6	B
Munshari	30.066	80.237	2201	19.145	25.093	12.748	75.06	A
Patti	29.407	79.931	1667	4.713	9.108	3.928	86.79	A
Pithoragarh	29.579	80.207	1538	60.489	60.297	37.065	57.39	A
Roorkee	29.866	77.901	243	3.519	4.615	1.556	281.5	C
Rudraprayag	30.287	78.983	859	7.741	6.335	3.654	191.0	A
Tanakpur	29.074	80.112	265	12.412	11.191	7.795	88.7	C
Tehri	30.374	78.430	1894	6.483	5.922	4.093	243.9	A
Udhamsingh	28.997	79.403	213	10.977	8.253	5.574	151.2	C
MPGO	30.530	78.747	1868	10.831	12.357	4.986	223.0	C
Delhi (LDR)	28.590	77.220	228	1.786	1.848	1.279	365.5	C

Table 2. Strong motion instrument characteristics

Agency	Recorder (digitizer)			Accelerometer (sensor)			
	Name	Bit	Dynamic range (db)	Name	Dynamic range (db)	Natural frequency (Hz)	Frequency range (Hz)
WIHG ^a	Syscom	16	96	MS 2004+	>110	>500	DC-150
IITR ^b	GSR-18	18	108	AC-63	>120	>200	DC-100
	GeoSig			Geosig			

^aWadia Institute of Himalayan Geology, Dehradun. ^bIndian Institute of Technology Roorkee²³.

2011 western Nepal earthquake (M 5.7) is close to the India–Nepal border. The data of 23 stations (Table 1) of this network were downloaded from the website²⁵ and utilized for analysis. All the stations are towards west and close to the epicentre of the earthquake. Figure 3 shows the waveform data recorded at two stations of this network during the occurrence of the western Nepal earthquake (M 5.7). These stations are Dharchula and Chamoli located at epicentre distances 37 and 168 km respectively.

In addition, the Wadia Institute of Himalaya Geology (WIHG), Dehradun, has also installed one strong motion recorder at Ghuttu. The station is located within the above-mentioned network however it is a part of the Multi-Parametric Geophysical Observatory (MPGO) at Ghuttu, Garhwal Himalaya, where 11 geophysical equipment have been installed for earthquake precursory research²⁶. In 2007, these continuous multi-component geophysical observations at a single site in India were started for the first time at Ghuttu by WIHG. At this station the strong motion data are being collected in trigger mode at 200 SPS using digital accelerometer. The

MS2004 + force-balance accelerometer of SYSCOM Instruments of Switzerland was installed in 2007, which is an analog force feedback triaxial accelerometer with natural frequency more than 500 Hz (Table 2). It can measure $\pm 1 g$ with frequency–amplitude response from 0 to 150 Hz and dynamic range 110 dB. This equipment was also triggered at the time of occurrence of the Western Nepal earthquake (M 5.7), which is located at a distance of 222 km. Figure 3c shows the waveform data of three components of this station.

At this station of MPGO, superconducting gravimeter (SG) is also installed which records continuous temporal variation of gravity for only the vertical component. These variations of acceleration due to gravity are the records of low frequency (<1 Hz); however, detection sensitivity is very high. SG is a highly sensitive instrument, the first equipment of the Indian continent²⁷, which records gravity variation to sub μGal level ($1 \mu\text{Gal} = 10^{-8} \text{ m/s}^2$) at a sampling rate of 1 SPS. Its data are influenced by tidal forces, atmospheric pressure and hydrological effects²⁶. After successfully removing these effects,

the co-seismic changes are visible in gravity values at the time of occurrence of local earthquakes of $M \geq 5$.

Earthquake source parameters

The earthquake which occurred on 4 April 2011 was located at the Nepal–India border in the western part of Nepal. The hypocentre obtained from the earthquake hazard programme of the US Geological Survey (USGS) is $29.678 \pm 9.9^\circ\text{N}$ and $80.750 \pm 8.9^\circ\text{E}$ at a focal depth of 12.5 ± 2.8 km. The India Meteorological Department (IMD), New Delhi evaluates the earthquake source parameters occurring in the Indian continent and surrounding regions. In addition, the USGS has also reported the focal mechanism solution that suggests subsurface deformation due to thrusting mechanism. The Global CMT solution is available for this event with similar focal mechanism of thrust deformation; however, the focal depth is deeper. Table 3 gives the available parameters of all these agencies. One fault plane of the obtained focal

mechanism of the USGS is dipping towards NNE having strike direction parallel to the MCT. The focal depth 12.5 km at this point suggests that the deformation occurred at the subsurface extension of the MCT and that is close to the junction of this tectonic fault with the detachment zone coinciding with Indian plate. Similar observations were observed during the occurrence of the 2007 Kharsali earthquake (M_w 5.0)². The two earlier strong earthquakes to the western part of its epicentre zone (Figure 2) indicate that thrust tectonics exists mainly in this part of the Himalaya and the source locations of these earthquakes are near the detachment zone, which is the general trend in the Himalaya.

Attenuation relation based on strong motion data

The seismic wave attenuation analysis using strong motion data is found helpful for better understanding of the seismic hazard scenario of the site. The attenuation behaviour of strong wave sheds light on the nature and extent of seismic wave propagation for both local and regional earthquakes. These attenuation characteristics are mainly formulated using strong motion data recorded by the accelerometer for moderate to large magnitude earthquakes. The 4 April 2011 Western Nepal earthquake (M 5.7) was strongly felt in the Central Himalayan region covering Nepal along with parts of India and Tibet. The earth vibrations were very strong, which have been well recorded even by the accelerograph installed at New Delhi about 365 km away from the epicentre. This valuable strong motion dataset was processed to obtain the attenuation characteristics for the central part of the Himalaya.

First of all, the strong motion dataset underwent regression analysis upon the existing attenuation relations of different region^{17,18} to obtain a well-matched relation for the present study region. The earthquake parameters (magnitude, epicentre distance and focal depth) of the existing relations were kept intact while the coefficients related to these parameters were changed to check the suitability of the relation for the present dataset. The best fit was obtained in each case to obtain new coefficients using recent data and then the newly developed parameters were used for inserting the theoretical curve. Based on each modified/developed theoretical curve, the residual was obtained from the recorded dataset to assess the suitability of the modified relation. It was observed that the relation developed¹⁷ for the Himalayan region had the highest acceptability and thus further regression analysis was performed to refine the relation using the current dataset. The theoretical regression attenuation relation adopted for analysis is as follows:

$$\log(A) = a_1 + a_2 * M - a_3 \log(D + e^{a_4 * M}), \quad (1)$$

where M is the magnitude of the earthquake, D the hypocentre distance (km) and A is the PGA relative to g

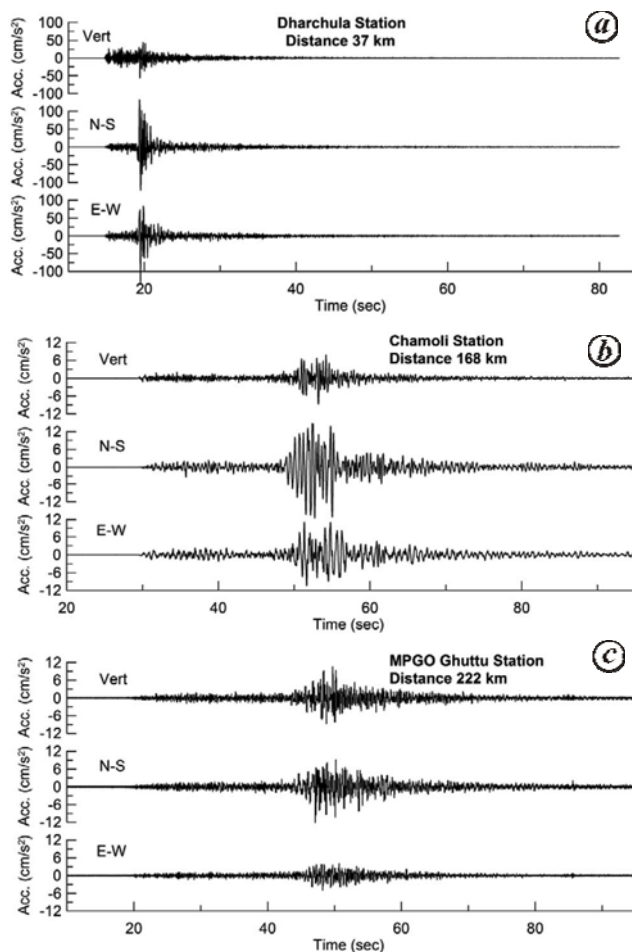


Figure 3. Accelerogram waveform data recorded at three stations of NW Himalaya: (a) Dharchula, epicentre distance 37 km; (b) Chamoli, epicentre distance 168 km; (c) MPMO Ghuttu, epicentre distance 222 km.

Table 3. Earthquake source parameters reported by different agencies

Agency	Date YY : MM : DD	Time H : min : s	Latitude (°N)	Longitude (°E)	Depth (km)	Magnitude	NP1			NP2		
							ST	DP	RK	ST	DP	RK
IMD ^a	2011 : 04 : 04	11 : 31 : 40.0	29.60	80.8	10.0	ML 5.7						
USGS ^b	2011 : 04 : 04	11 : 31 : 46.6	29.68	80.75	12.5	M_w 5.4	307	48	111	98	46	69
GCMTC ^c	2011 : 04 : 04	11 : 31 : 44.3	29.43	80.71	18.8	M_w 5.4, M_b 5.6	318	30	128	96	67	70

USGS, United States Geological Survey; IMD, India Meteorological Department; NP1, Nodal Plane 1; NP2, Nodal Plane 2; ST, Strike; DP, Dip; RK, Rake. ^aIndia Meteorological Department (<http://www.imd.gov.in>). ^bNEIC USGS catalogue (<http://earthquake.usgs.gov/regional/neic/>). ^cGlobal Centroid Moment Tensor (<http://www.globalcmt.org>).

(acceleration due to gravity, 9.80 m/s^2). The regression coefficients are a_1 , a_2 , a_3 and a_4 .

The analysis performed on eq. (1) using recent dataset has resulted in new coefficient (constant) values which are a little different compared to the obtained values¹⁷. The new values inserted in eq. (2) suggest minimum residual for this earthquake. The obtained attenuation relation is as follows:

$$\log(A_{\text{Horz}}) = -1.207 + 0.363 * M - 1.206 \log(D + e^{0.480 * M}). \quad (2)$$

Here M , the magnitude of the earthquake (5.7) is constant and the hypocentral distance is changed to obtain A , the average PGA for horizontal components on all the recording stations. Table 1 provides the recorded PGA values of different stations.

The newly developed attenuation curve is plotted in Figure 4 along with the recorded data and the attenuation curves of other regions. The attenuation curve for the present study region is for M 5.7 (dotted line), while for other regions it is for three magnitude sizes as M 5.0, M 5.7 and M 6.0 (solid lines). Also, based on the obtained attenuation relation (eq. (2)), the curves formulated for three magnitude scales M 5.0, M 5.7 and M 6.0 are plotted (Figure 5). The recorded values of two horizontal components and their average values are superimposed on these curves to compare the results with the observed values. The obtained attenuation relation is a nonlinear function indicating high attenuation of the acceleration with distance that accounts for multiple factor effects.

Discussion and conclusion

The seismic hazard analysis is an appropriate approach utilizing strong motion data at the time of occurrence of M 5.0 and larger earthquakes. The database used for present study is the ground acceleration motion recorded in the central part of the Himalaya during the occurrence of the M 5.7 earthquake on the western border of India–Nepal. The attenuation patterns of seismic waves propagating within the subsurface of the earth were formulated for better seismic hazard analysis. The structural heterogeneities beneath the Central Himalaya may have immense control on the extent of seismic wave propaga-

tion and thereby influence the pace of seismic attenuation because of the varying amount of various causative factors associated with the subsurface media in the form of either material intrusives or extrusives, or cracks or fractures, or a combination of all these as witnessed for diverse seismotectonic regions elsewhere in the world^{28,29}. The relations can be used for the evaluation of source size of future strong earthquakes, site amplification and properties of propagation path. These data-originated relations are region-specific, very important and require to be modified and improved after the occurrence of each strong earthquake. The formulated relations are non-linearly related with the epicentre distance and the earthquake size which may be different for different seismogenic zones. The relations may vary for regions such as the Himalaya due to high variation in strata³, both in the horizontal and vertical directions. Moderate to large earthquakes are able to excite the strong motions, oscillations recorded on the earth's surface. The frequency of occurrence of these earthquakes is low, which decreases with increasing magnitude. Hence longer period of observation is required making each earthquake an important entity. Determination of attenuation relations using M 5.7 Nepal earthquake of 4 April 2011 is useful for the refinement of existing relations of the Central Himalaya.

The strong motion data of local array of the central part of the Himalaya have been used^{19,22}; the stations are mainly towards west and adjacent to the epicentre (Figure 1) of M 5.7 located in western Nepal. The acceleration records of three stations for a total period of about 100 sec are shown in Figure 3, which also include some parts of pre-event data. It is visible that the oscillation amplitude of strong motion and its PGA value are extremely variable with distance; the vertical scale of the nearest station (Dharchula at 37 km distance) is different compared to two other stations.

The attenuation relation of any region is obtained using the data of many earthquakes of different magnitude range, i.e. $M \geq 5.0$. In the present study, the previously developed relation of different regions are assessed for obtaining a relation close to the present data. In the first step of analysis, average PGA values of horizontal components are plotted along with the attenuation curves of

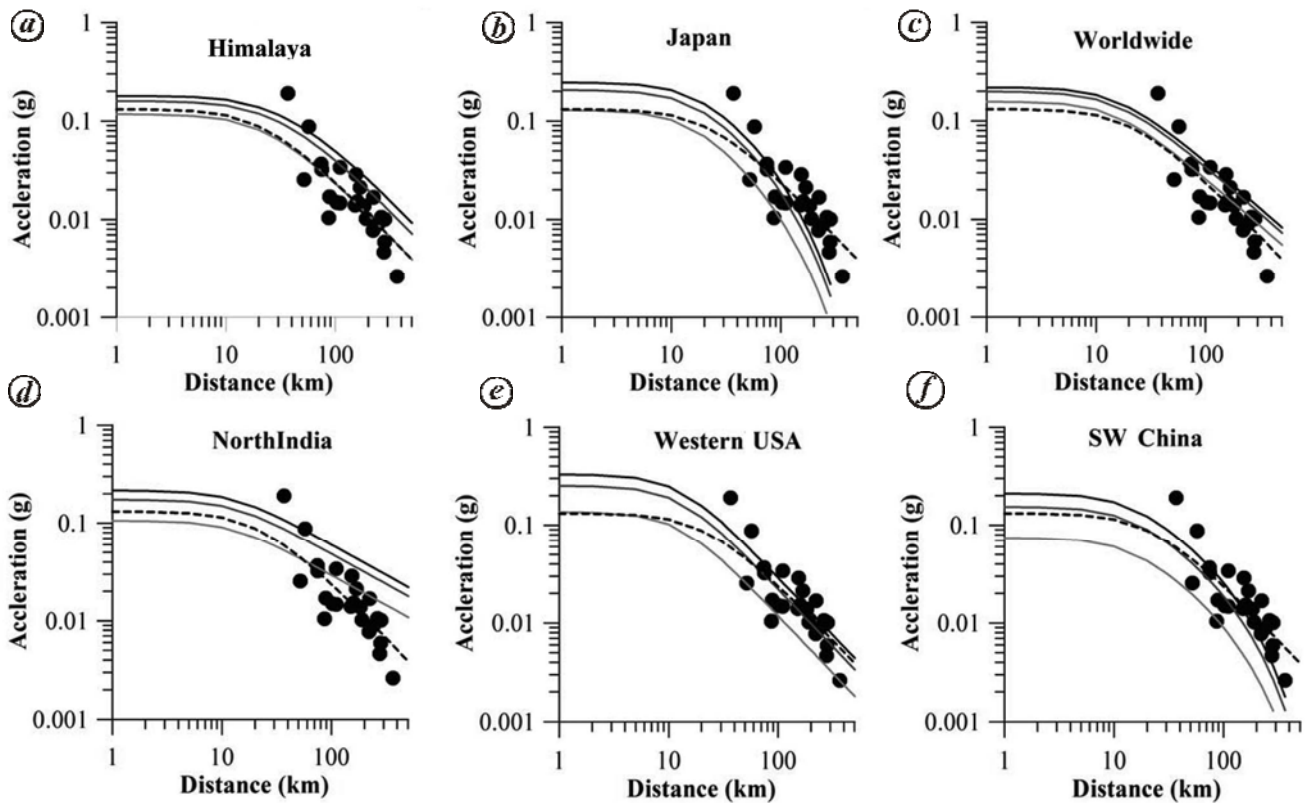


Figure 4. Attenuation curves of different regions of the world based on the previous developed relations^{17,18}. The curves for M 6.0, M 5.7 and M 5.0 are shown with solid line. The present peak ground acceleration (PGA) data of horizontal component are shown with filled circles, while dotted line denotes attenuation relation for recent data of M 5.7. (a) Himalaya; (b) Japan; (c) worldwide; (d) North India; (e) Western USA; (f) SW China.

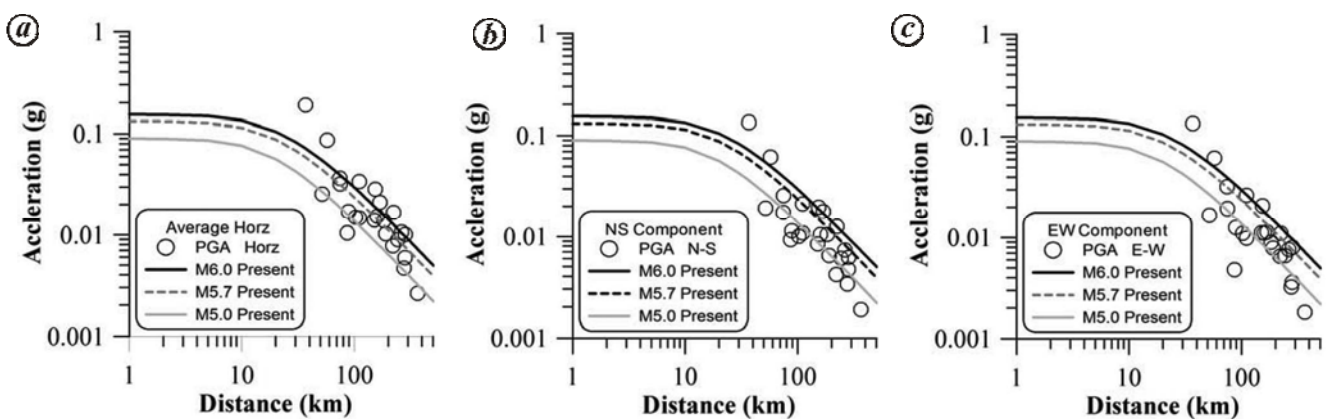


Figure 5. PGA values of horizontal components plotted as circles. The incorporated curves for M 6.0 (solid line), M 5.7 (dotted line) and M 5.0 (solid line) are also shown. (a) Vertical component; (b) NS horizontal component; (c) E-W horizontal component.

different regions. Figure 4 is the resultant plot for comparison of datasets. The present dataset is scattered and the observed values deviate from the attenuation curves of other regions. Therefore, we plotted attenuation curves for three magnitudes M 5.0, M 5.7 and M 6.0; even then, few values are far away from these curves. The attenuation curve obtained using these data for M 5.7 is shown with dotted line in Figure 4 and the curves of different regions for M 5.0, M 5.7 and M 6.0 are plotted with solid

lines. Examination of these plots suggests that attenuation curves of the Himalaya obtained based on data of seven previous earthquake are in close agreement compared to others¹⁸. However, the present data do not fit well with the curves developed for Northern India (Figure 4d)¹⁷. Instead, the data show a good relation with the curves reported for worldwide data (Figure 4c)¹⁶ and that of western USA (Figure 4e)¹⁵. The curves of other regions (Japan, SW China) are different, suggesting the role of analogous

geo-tectonic settings or the nature of the subsurface structural heterogeneities of the media through which the seismic wave propagates.

It is observed that the recorded data are scattered at some sites away from the theoretical curves in each plot, particularly at two nearest stations (Dharchula and Pithoragarh). Therefore, the recent data are not in full agreement with the curves developed for other regions, but close to the relation formulated¹⁸. It has been mentioned in the previous section that the already developed attenuation relation for the Himalaya is utilized to develop the relation for the Central Himalaya after calculating new coefficients based on regression analysis. The modified coefficients (a_1 – a_4) from the present study are –1.207, 0.363, 1.206 and 0.480 respectively for the Central Himalaya compared to initial values –1.072, 0.3903, 1.21 and 0.5873 respectively, for the Himalaya¹⁸. On the basis of modified relation (eq. (2)), the theoretical curves are inserted for M 5.0, M 5.7 and M 6.0 for further analysis. These curves are plotted in Figure 5. The attenuation curve mainly resembles the average value on which it was formulated. However, few datapoints are beyond M 6.0 on the higher side and M 5.0 towards the lower side. The deviation of these values from the theoretical curve may be due to heterogeneity in the crustal composition and also the earthquake source mechanism. In horizontal extent, the Himalayan region is divided into geological zones comprising different composition³. The coordinates of source mechanism (strike, dip and slip) and the type of mechanism (thrust in the present case) may also influence the data. In general, the data indicate that attenuation trend is different for closer stations up to 120–150 km compared to distant stations; the maximum distance of the dataset is 365 km. These two different trends point out a sudden change in the subsurface structure; the closer stations define the property of uppermost structure of the lithosphere, while the distant stations of the lower part. The changes in the attenuation curves for the Himalayan region are dependent on the Moho depth¹⁹ and the discrepancy of this trend may be the cause of deviation of the obtained theoretical relations from the actual values.

The formulated attenuation relation (eq. (2)) is further utilized to measure the deviation of each recorded value from the theoretical value. The large deviation may account for the Moho depth variation¹⁹, which changes abruptly in the present study region of the Himalaya. Similar to topography (Figure 1), the Moho depth is less in the Indo-Gangetic plain close to the HFT and more in the Higher Himalaya, north of MCT. It may also account for the directive effect of the earthquake source rupturing effect; this effect will be high near the source. The rupture of the source zone takes place along a plane; therefore stations close to the boundary of the plane experience strong vibrations irrespective of the hypocentre distance. The directive effect takes a rectangular form near the source, changing to cylindrical form and

then circular form with increasing distance. Therefore, far away from the source the effects is nullified. However, in the heterogeneous region where the geological and tectonic elements show drastic variation, there may be maximum deviation in the source geometry. Figure 6 shows observed deviation, the data recording stations are plotted with open rectangle. The difference in observed PGA values from the theoretical values varies between 0.13 and –0.02 g . A higher value of 0.13 g deviation is recorded at the nearest station (Dharchula; Figure 6). This station is towards the NW end of the strike obtained from the focal mechanism of the USGS. The greater difference may be the effect of directivity based on rupture fault of the earthquake source. This station is on the hanging-wall and therefore it may be considered that the subsurface tectonic deformation occurred due to thrusting of the higher Himalaya upon the lesser Himalaya along the MCT. The focal mechanism also favours this and hence there may be some enhancement of vibrations for stations located on the hanging wall. Irrespective of this, the two stations on the foot-wall have the lowest values and this may be partly due to directivity effect and partly the strata property under stations. The contours formed through this deviation give a pictorial view (Figure 6) that also matches with the tectonic elements (Figure 3). This observation highlights the variation of geo-tectonic set-up of the region. However, the enhancement of PGA values also depends on the site conditions of the recording station. The trend for the distant stations is not clear; however, the trends of both the near and distant stations are similar and perpendicular to the existing strike of the major tectonic (HFT, MBT, MCT and STD) features of the region.

The ratio of the horizontal and vertical components of the observed PGA values was also obtained to evaluate the seismic hazard at each station. Figure 7 shows the variation for each horizontal component (NS and EW) and for the average of both. The calculated H/V ratios are

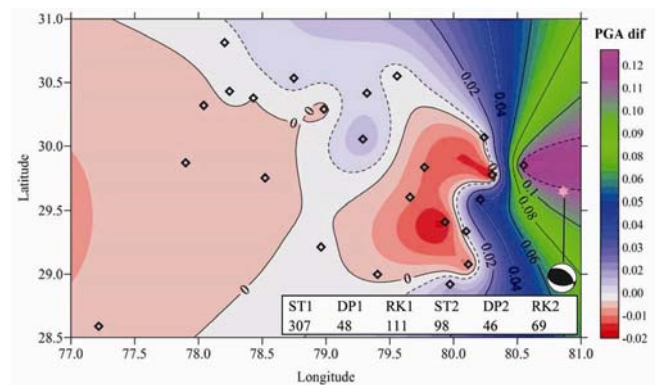


Figure 6. Deviation of recorded PGA values from the obtained attenuation characteristic curve at specific distance plotted for vertical component data. Star denotes the epicentre location; the focal mechanism solution of USGS is plotted and its parameters are also mentioned.

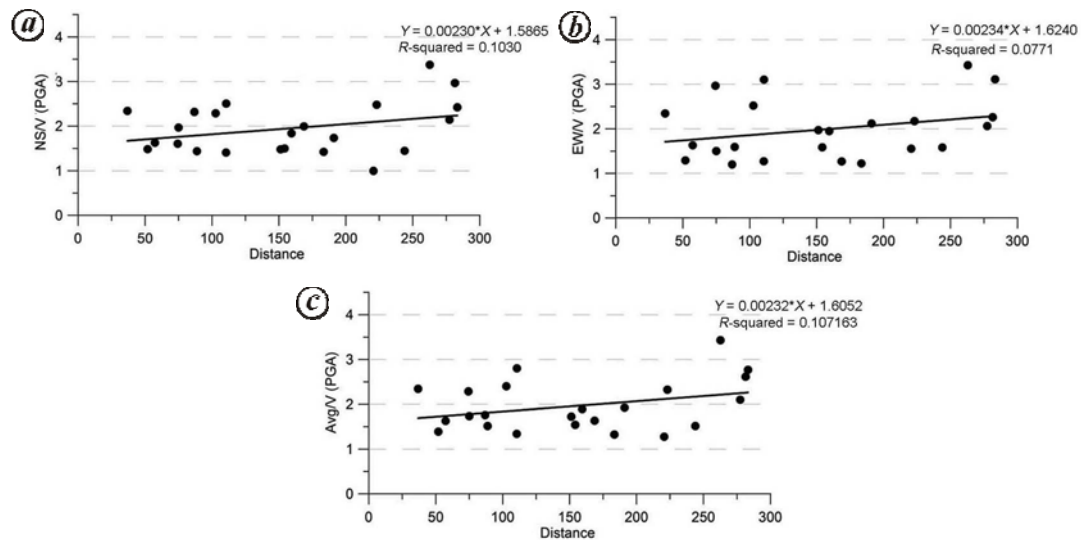


Figure 7. The variation of horizontal to vertical (H/V) ratio observed for the PGA data with epicentre distance for (a) NS horizontal component; (b) E–W horizontal component; (c) average values of the two horizontal components.

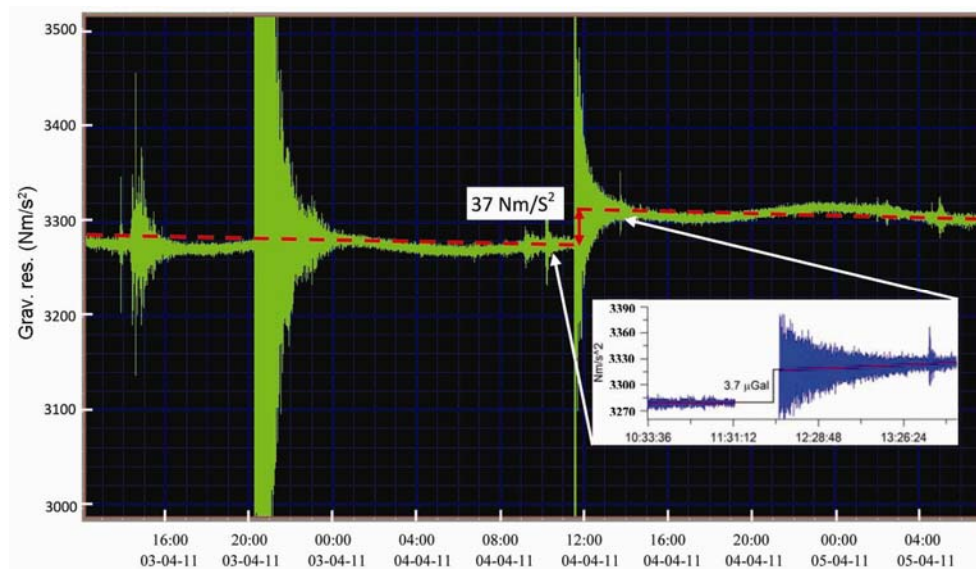


Figure 8. Co-seismic offset of $3.7 \mu\text{Gal}$ observed in the superconducting gravimeter data of MPGO Ghuttu during the $M 5.7$ Nepal earthquake of 4 April 2011.

between 1.0 and 3.5, and most of the values are less than 2.0; the high value suggests high vulnerability during the earthquake. This observation clearly indicates that the PGA values are higher in case of horizontal component compared to vertical component. Although the trend is not clear, linear regression relations were used to observe the behaviour with increasing distance. The obtained regression coefficients (R -squared values given in Figure 7) indicate a poor relation; the obtained relation suggests that the ratio increases with increase in distance. This observation also suggests that the nearer stations (up to 120 km) and the distant stations have different trends. Only one station has the highest value more than 3, suggesting highest vulnerability. Four stations close to the

epicentre and five distant stations have values between 2 and 3; the other values are less than 2. It is observed that the stations located on thick soil have with high values.

During this earthquake, the earth vibrations exerted strong variation in the gravity data recorded by the SG equipment installed at 222 km at MPGO, Ghuttu. The analysis of continuous records of gravity indicates a sudden offset, that is, the co-seismic change ($3.7 \mu\text{Gal}$) occurred at the origin time of the earthquake (Figure 8). The detailed procedure of detection of co-seismic change has been discussed by Kumar *et al.*²⁶ is based on a method developed for SG data during the occurrence of $M 8.0$ earthquake³⁰. In the same line of observations, Kim *et al.*³¹ have also reported co-seismic changes in gravity

using SG data and also Kumar *et al.*³² observed sudden shift of 5.2 μgal at the time of occurrence of M_w 5.0 earthquake located at about 60 km distance using SG data of this station. At MPMO, Ghuttu the continuous recording using SG was started in 2007, which indicates that co-seismic change takes place at the time of occurrence of $M \geq 5.0$ earthquake within a distance of ~ 200 km. Therefore, the recent earthquake was a strong event in this central part of the Himalaya and the shaking was reported far away, i.e. more than 1000 km. A recent work on PGA for the Himalayan region³³ indicates high vulnerability for the present study region.

- Bollinger, L., Perrier, F., Avouac, J. P., Sapkota, S., Gautam, U. and Tiwari D. R., Seasonal modulation of seismicity in the Himalaya of Nepal. *Geophys. Res. Lett.*, 2007, **34**, L08304.
- Kumar, N., Paul, A., Mahajan, A. K., Yadav, D. K. and Bora, C., The M_w 5.0 Kharsali, Garhwal Himalayan earthquake of 23 July 2007: source characterization and tectonic implications. *Curr. Sci.*, 2012, **102**, 1674–1682.
- Valdiya, K. S., Structural set-up of the Kumaun Lesser Himalaya – Colloqu Intern CNRS, 268, Ecologie et Geologie de l’Himalaya, Paris, 1976, pp. 449–462.
- Upreti, B. N., An overview of the stratigraphy and tectonics of the Nepal Himalaya. *J. Asian Earth Sci.*, 1999, **17**, 577–606.
- Hodges, K. V., Tectonics of the Himalaya and southern Tibet from two perspectives. *Geol. Soc. Am. Bull.*, 2000, **112**(3), 324–350.
- Ni, J. and Barazangi, M., Seismotectonics of the Himalayan collision zone: geometry of under thrusting Indian Plate beneath the Himalaya. *J. Geophys. Res.*, 1984, **89**, 1147–1163.
- Bilham, R., Gaur, V. K. and Molnar P., Himalayan seismic hazard. *Science*, 2001, **293**, 1442–1444.
- Sapkota, S. N., Bollinger, L., Klinger, Y., Tapponnier, P., Gaudemer, Y. and Tiwari, D., Primary surface ruptures of the great Himalayan earthquakes in 1934 and 1255. *Nature Geosci.*, 2013, **6**, 71–76.
- Mishra, O. P., Intricacies of the Himalayan seismotectonics and seismogenesis: need for integrated research. *Curr. Sci.*, 2014, **106**(2), 176–187.
- Molnar, P. and Tapponnier, P., Active tectonics of Tibet. *J. Geophys. Res.*, 1978, **83**, 5361–5375.
- Gitis, V., Yurkov, E., Arora, B. R., Chabak, S., Kumar, N. and Baidya, P., Analysis of seismicity in North India. *Russ. J. Earth Sci.*, 2008, **10**, 1-11 ES5002; doi: 10.2205/2008ES000303
- Molnar, P. and Lyon-Caen, H., Fault plane solutions of earthquakes and active tectonics of the Tibetan Plateau and its margins. *Geophys. J. Int.*, 1989, **99**, 123–153.
- Gahalaut, K. and Rao, N. P., Stress field in the western Himalaya with special reference to the 8 October 2005 Muzaffarabad earthquake. *J. Seismol.*, 2009, **13**, 371–378.
- Paudyal, H., Shanker, D., Singh, H. N., Panthi, A., Kumar, A. and Singh, V. P., Current understanding of the seismotectonics of western Nepal Himalaya and vicinity. *Acta Geod. Geoph. Hung.*, 2010, **45**(2), 195–209; doi: 10.1556/AGeod.45.2010.2.5
- McGuire, R. K., Seismic ground motion parameter relations. *J. Geotech. Eng. Div. ASCE*, 1978, **104**, 481–490.
- Campbell, K. W., The dependence of peak horizontal acceleration on magnitude, distance, and site effects for small-magnitude earthquakes in California and eastern North America. *Bull. Seismol. Soc. Am.*, 1989, **79**, 1311–1346.
- Kumar, D., Toetia, S. S. and Khattri, K. N., The representability of attenuation characteristics of strong ground motions observed in the 1986 Dharmasala and 1991 Uttarkashi earthquakes by available empirical relations. *Curr. Sci.*, 1997, **73**, 543–547.
- Sharma, M. L., Attenuation relationship for estimation of peak ground horizontal acceleration using data from strong-motion arrays in India. *Bull. Seismol. Soc. Am.*, 1998, **88**(4), 1063–1069.
- Parvez, I. A., Gusev, A. A., Panza, G. F. and Petukhin, A. G., Preliminary determination of the interdependence among strong motion amplitude, earthquake magnitude and hypocentral distance for the Himalaya region. *Geophys. J. Int.*, 2001, **144**, 577–596.
- Campbell, K. W., Strong motion attenuation relations: a ten-year perspective. *Earthquake Spectra*, 1985, **1**, 759–804.
- Joshi, J., Analysis of strong motion data of the Uttarkashi earthquake of 20 October 1991 and the Chamoli earthquake of 28 March 1999 for determining the Q value and source spectra parameters. *ISER J. Earth Technol.*, 2006, **468**(43), 11–29.
- Kumar, A., Mittal, H., Sachdeva, R. and Kumar, A., Indian strong motion instrumentation network. *Seismol. Res. Lett.*, 2012, **83**(1), 59–66.
- Mittal, H., Kumar, A. and Rebecca, R., Indian strong motion instrumentation Network and its site characterization. *Int. J. Geosci.*, 2012, **3**(6), 1151–1167.
- Malik, S., Sharma, M. L. and Khandelwal, D. D., Estimation of spectral strong ground motion for North East India using PSHA. In 13th Symposium on Earthquake Engineering, Roorkee, 18–20 December 2006, pp. 137–147.
- www.pesmos.in
- Kumar, N., Rawat, G., Choubey, V. M. and Hazarika, D., Earthquake precursory research in western Himalaya based on the Multi-Parametric Geophysical Observatory data. *Acta Geophys.*, 2013, **61**(4), 977–999; doi: 10.2478/s11600-013-0133-1
- Arora, B. R., Kamal, Kumar, A., Rawat, G., Kumar, N. and Choubey, V. M., First observations of the earth from Indian Super conducting Gravimeter in the Himalaya. *Curr. Sci.*, 2008, **95**(11), 1611–1617.
- Mishra, O. P., Zhao, D. and Singh, D. D., Northwest Pacific fundamental mode Rayleigh-wave group velocity and its relationship with tectonic structures. *Bull. Seismol. Soc. Am.*, 2005, **95**(6), 2125–2135.
- Mishra, O. P., Crustal heterogeneity in bulk velocity beneath the 2001 Bhuj earthquake source zone and its implications. *Bull. Seismol. Soc. Am.*, 2013, **103**(6), 3235–3247.
- Imanishi, Y., Sato, T., Higashi, T., Sun, W. and Okubo, S., A network of superconducting gravimeters detects submicrogal coseismic gravity changes. *Science*, 2004, **306**, 476–478.
- Kim, J. W., Neumeier, J., Kim, T. H., Woo, I., Park, H. J., Jeon, J. S. and Kim, K. D., Analysis of superconducting gravimeter measurements at MunGyung Station, Korea. *J. Geodyn.*, 2009, **47**, 180–190.
- Arora, B. R., Rawat, G., Kumar, N. and Choubey, V. M., Multi-Parametric Geophysical Observatory: gateway to integrated earthquake precursory research. *Curr. Sci.*, 2012, **103**, 1286–1299.
- Parvez, I. A., Nekrasova, A. and Kossobokov, V., Estimation of seismic hazard and risks for the Himalayas and surrounding regions based on unified scaling Law for earthquakes. *Nat. Hazards*, 2014, **71**(1), 549–562.

ACKNOWLEDGEMENTS. We thank the Director, WIHG, Dehradun for permission to publish this manuscript. Dr Ashok Kumar (IITR) for running a good network of strong motion data in the Central Himalaya under a sponsored project of MoES, New Delhi, and the MPMO team of WIHG for collecting continuous data through a MoES, New Delhi sponsored project (MoES/P.O. (Seismo)/NPEP(15)/2009).

Received 24 February 2015; revised accepted 28 July 2015

doi: 10.18520/v109/i10/1822-1830